PERGAMON

International Journal of Heat and Mass Transfer 42 (1999) 3447–3459

International Journal of HEAT and MASS TRANSFER

Enhancement of condensate drainage from a horizontal integral-fin tube by means of a solid strip

Marian Trela*, Dariusz Butrymowicz

Institute of Fluid-Flow Machinery, Polish Academy of Sciences, Gen. J. Fiszera 14, PL 80-952 Gdańsk, Poland

Received 16 February 1998; received in revised form 21 December 1998

Abstract

This paper describes the process of intensification of condensation heat transfer on a single horizontal integral-fin tube due to the enhancement of condensate drainage. An analytical model of the drainage effect of a special longitudinal solid strip is presented. The so-called drainage parameter seems to be the most important in the model. Exemplary calculations have been made to investigate the effect of tube and strip geometry on the enhancement of the drainage process. The experimental investigations of the condensate drainage from a single horizontal integral-fin and unfinned tube by using a longitudinal solid drainage strip are presented in this paper. The condensation heat-transfer augmentation in the range 6–25% was achieved by means of a solid drainage strip.

1. Introduction

In recent years, there has been a growing interest in using enhanced heat transfer surface, i.e. low profile fins, in refrigerating and heat pump condensers. However, integral fin tubes, which are available from manufacturers with the fin density varying from about 350 to approximately 2000 fins per metre, are thought to be unsuitable for some cases. It is well known that when a horizontal finned tube comes in contact with a highly wetting liquid, surface tension force will cause the liquid to be retained between the fins at the bottom of the tube. This phenomenon is known as liquid 'hold-up', 'retention' or 'flooding'. Based on their own results, Webb et al. [1] concluded that the heat transfer rate across the zone of retained condensate is negligible for most practical cases. Most of the available experimental data gathered from systematic tests with the family of finned tubes [2,3] and analytical models [4] suggest that as the spacing between fins decreases, the heat transfer coefficient based upon the smooth tube surface area increases to a maximum value at a certain fin spacing. Further decrease in fin spacing below this optimum value results in a strong decrease in heat transfer, principally due to increased flooding between the fins.

Condensate retention between the fins was studied by many investigators, e.g. [5,6]. The flooding may be characterised by the so-called flooding angle Φ measured circumferentially from the top of the tube to a position at which the entire fin flanks are completely covered with retained liquid. The flooding angle depends mainly on the tube geometry and the capillary constant.

Two kinds of the drainage strips are known—porous drainage strip and solid drainage strip. The porous strip drives the condensate into its pores and creates a low pressure region within the liquid at the bottom of the tube. This principle is commonly used in heat pipe wicks where the pressure difference across the liquid–

* Corresponding author.
E-mail address: mtr@imppan.imp.pg.gda.pl (M. Trela)

0017-9310/99/$ - see front matter
PII: S0017-9310(99)00034-4

Nomenclature

a	capillary constant, $a=[\sigma/(\rho g)]^{1/2}$; coefficients in Eq. (10)
c_p	specific heat
C	coefficients in Eq. (36)
Ca	capillary number, $Ca=\mu\bar{u}_N/\sigma$
D	fin tip diameter
Fr	Froude number based on Nusselt film thickness, $Fr=\bar{u}_N^2/(g\delta_N)$
Fr_a	Froude number based on capillary constant, $Fr_a=\bar{u}_N^2/(ga)$
g	acceleration of gravity
Ga	Galileo number, $Ga=gD^3/\nu^2$
h_{fg}	specific enthalpy of evaporation
H_{ac}	dimensionless active height of the strip
H_f	fin height
K	dimensionless film curvature, $K=\kappa a$, see also Eqs. (31)
Ku	Kutateladze number, $Ku=h_{fg}/(c_p\Delta T)$
Nu	Nusselt number, $Nu=\alpha D/\lambda$
p	pressure
P	dimensionless pressure gradient, $P=\lvert dp/dx\rvert/(\rho g)$
P_f	fin pitch
Pr	Prandtl number, $Pr=c_p\mu/\lambda$
Re	Reynolds number, $Re=2\Gamma/\mu$
t	drainage strip thickness
u, v	velocity components in the x- and y-direction, respectively
$\bar{u}_N$	average x-component of velocity based on Nusselt film thickness, $\bar{u}_N=\delta_N^3 g/(3\nu)$
W_t	fin spacing at fin tip
We	Weber number, $We=\rho\bar{u}_N^2\delta_N/\sigma$
x, y	co-ordinates
X	dimensionless co-ordinate, $X=x/a$
Y	function defined by Eq. (15).

Greek symbols

α	heat-transfer coefficient based on the smooth tube area of the diameter D
α, β, γ	dimensionless parameters, Eq. (12a)
Γ	overall mass flow rate per unit length
δ	condensate film thickness
δ_N	Nusselt film thickness, $\delta_N=[3\Gamma\nu/(2\rho g)]^{1/3}$
Δ	dimensionless condensate film thickness, $\Delta=\delta/\delta_N$
ΔT	mean vapour-to-surface temperature difference
ε	dimensionless parameter, defined by Eq. (30a)
ε_d	drainage parameter, defined by Eq. (30b)
θ	fin tip half angle
θ_w	contact angle
κ	film curvature
λ	thermal conductivity
μ	dynamic viscosity
ν	kinematic viscosity
ρ	density
σ	surface tension
τ	dimensionless drainage strip thickness, $\tau=t/2a$
Φ, Φ_f	flooding angle, $\Phi_f=\Phi/\pi$
χ	real root of Eq. (20)
ψ	stream function
Ω	coefficient of heat transfer intensification due to the fin geometry.

Subscripts

c	interfin channel
D	tube
f	fin; flooding
h	hydrostatic region
M	maximum
O	tangent
s	strip; saturation
st	starting point of numerical solution.

vapour interface pumps the liquid from one end of the pipe to the other. A theoretical model of the flooding angle for the finned tube fitted with the porous drainage strip was developed by Honda and Nozu [7].

Some experimental investigations of steam condensation on finned tubes with solid drainage strips were presented by Marto et al. [8]. The maximum increase of the heat transfer coefficient during film condensation was 35%, compared to that of the tube without a strip. Experimental investigations with solid drainage strips for a horizontal finned tube were carried out by Yau et al. [9]. It turned out that for steam as a condensing medium, a strip 8 mm in height provided only a slight increase of the heat transfer coefficient, compared to a strip 4 mm in height. A solid drainage strip 8 mm in height was also applied to intensify the condensation heat transfer at an unfinned tube by Yemielianov et al. [10]. A 20% increase of the heat transfer coefficient was achieved, compared to the unstripped tube. Honda and Nozu [7] investigated the process of condensation of methanol vapour in horizontal finned copper tubes for which a moderate increase of the heat transfer coefficient was observed as the flooding angle did not increase that much.

It is worth noting, that experimental investigations carried out in [7–10] favour the application of relatively high solid strips in the belief that in order to assure an appropriate drainage effect the strip should be high enough. However, the application of strips of 8–14 mm in height can be inconvenient as it necessitates increased spacing between the tubes. Honda and Nozu [7] proved experimentally that in the case of the porous strip the heat transfer enhancement is greater than for the solid strip of the same height. Due to these findings less attention has been paid so far to the solid strip. However, the solid strip also has some advantages. One of them is lack of sensitivity to impurities or oil concentration in the working fluid which might fill the pores and stop the beneficial action of the porous strip. Furthermore, the solid strip is cheaper and easier in practical application. On the other hand, lack of an analytical method to predict the 'suction' effect of the solid drainage strip causes strong difficulties in obtaining an appropriate strip geometry.

The purpose of this paper is to provide a theoretical model for the solid drainage strip. The model presented below is a modification of an earlier model developed by Butrymowicz and Trela [11]. It allows the calculation of the flooding angle and with the help of this quantity the determination of the heat transfer coefficient for the tube fitted with a solid strip. In particular, the effects of geometry of the solid strip and integral-fin tube can easily be established.

2. Theoretical approach

A sketch of the considered situation is presented in Fig. 1(a). A horizontal integral-fin tube is fitted with a solid drainage strip. Fig. 1(b) presents a cross-section of this tube. The flooding angle Φ is depicted there. As shown in the figure, the concave liquid meniscus forms near the junction of the tube and the strip.

The curvature of the condensate retained between

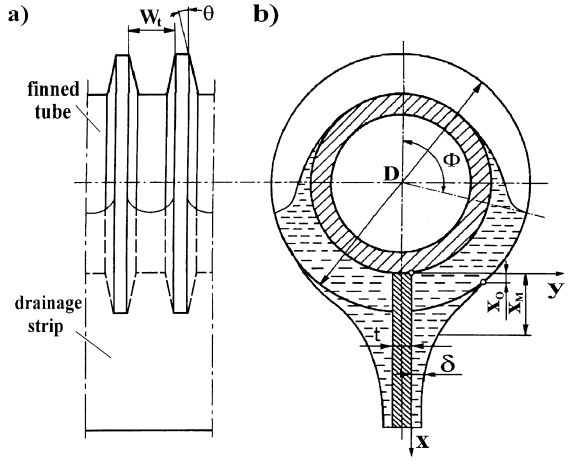

Fig. 1. The physical problem statement: (a) integral-fin tube fitted with the drainage strip; (b) cross-section of the tube.

the fins and of the liquid film flowing over the strip varies both in value and sign. It starts from a small negative value at a point of tangency x_O, reaches a maximum—positive value—at x_M and then diminishes to zero at infinity. The positive influence of the solid strip on the drainage process is therefore, caused by the above curvature distribution producing an effect of 'suction' beneath the finned tube.

The following simplifications are made in the analysis:

- It is assumed that no condensation occurs on the strip which is confirmed by the observation that at the higher part of the strip and at the very bottom of the tube the condensate layer is very thick.
- The interfin channels are completely filled with the condensate at the bottom of the tube.
- Changes of curvature along the tube are negligible.
- The strip is infinite in height. This assumption is very useful for the analysis of the condensate curvature distribution, however, the theory given below permits the calculation of the active height of the strip.
- The flow of the condensate is laminar.

Bearing in mind the simplifications listed above, the governing equations of momentum, continuity and pressure distribution for the strip are as follows:

$$u\frac{\partial u}{\partial x}+v\frac{\partial u}{\partial y}=g-\frac{1}{\rho}\frac{\partial p}{\partial x}+\nu\frac{\partial^2 u}{\partial y^2}, \tag{1}$$

$$\frac{\partial p}{\partial y}=0, \tag{2}$$

$$\frac{\partial u}{\partial x}+\frac{\partial v}{\partial y}=0, \tag{3}$$

$$p=p_s-\sigma\kappa, \tag{4}$$

where the film curvature κ is given by the well-known formula:

$$\kappa=\frac{\delta''}{(1+\delta'^2)^{3/2}},\quad (\,)'\equiv\frac{\mathrm{d}}{\mathrm{d}x}. \tag{4a}$$

The knowledge of the pressure distribution in the liquid phase along the strip is necessary in order to calculate the suction effect of the strip. However, this requires the distribution of the liquid meniscus curvature to be known. It is clear from Eq. (4a) that in order to obtain this curvature distribution one has to know the film thickness distribution along the strip. This problem is considered below.

The condensate surface $\delta=\delta(x)$ (Fig. 1(b)) is the stream surface. Hence, we have the streamline equation

$$\frac{\mathrm{d}x}{u}=\frac{\mathrm{d}y}{v}. \tag{5}$$

Introducing the stream function

$$u=\frac{\partial\psi}{\partial y},\quad v=-\frac{\partial\psi}{\partial x}, \tag{6}$$

the following equation is obtained from Eqs. (1)–(4)

$$\frac{\partial\psi}{\partial y}\frac{\partial^2\psi}{\partial x\,\partial y}-\frac{\partial\psi}{\partial x}\frac{\partial^2\psi}{\partial y^2}=g+\frac{\sigma}{\rho}\frac{\mathrm{d}\kappa}{\mathrm{d}x}+\nu\frac{\partial^3\psi}{\partial y^3}. \tag{7}$$

From Eq. (5) we have

$$\frac{\partial\psi}{\partial x}(x,\ y=\delta)=-\frac{\mathrm{d}\delta}{\mathrm{d}x}\frac{\partial\psi}{\partial y}(x,\ y=\delta). \tag{8}$$

The following boundary conditions are valid for Eq. (7)

$$\frac{\partial\psi}{\partial x}(x,\ y=0)=0,\quad \frac{\partial\psi}{\partial y}(x,\ y=0)=0,\quad \frac{\partial^2\psi}{\partial y^2}(x,\ y=\delta)=0. \tag{9}$$

The stream function is assumed to have the following form

$$\psi(x,\ y)=\sum_{i=0}^{n}a_i\left(\frac{y}{\delta(x)}\right)^i. \tag{10}$$

In order to satisfy the boundary conditions (9) and relation (8), the coefficients in Eq. (10) should be as follows:

$$n=3,\quad a_1=0,\quad a_2=\frac{3}{4}\frac{\Gamma}{\rho},\quad a_3=-\frac{1}{4}\frac{\Gamma}{\rho}. \tag{11}$$

Details about finding the coefficients (11) are described in [11]. Taking into account Eq. (7) with the coefficients (11), one can obtain the equation for the liquid film distribution written in the dimensionless form [11]

$$\Delta'''-3\alpha\Delta'\Delta''^2(1+\alpha\Delta'^2)^{-1}-(1+\alpha\Delta'^2)^{3/2}(\alpha^{-1/2}(\Delta^{-3}-1)-\beta\Delta^{-3}\Delta')=0, \tag{12}$$

where $\Delta\equiv\delta/\delta_N$ and

$$\alpha=\frac{We}{Fr},\quad \beta=\frac{3}{16}Re,\quad Re=\frac{4}{3}\gamma\alpha^{3/2},\quad \gamma=\frac{Fr_a}{Ca^2}. \tag{12a}$$

The dimensionless quantity γ depends merely on the physical properties of the condensate. On the other hand the dimensionless quantity α depends on the con-

densate flow rate, which must be calculated with the use of a separate model of heat-transfer on the finned tube. Thus, the link between the hydrodynamics and heat transfer is expressed by quantity α.

Taking into account the simplification used in this analysis, namely the assumption that the strip extends to infinity, the initial conditions for Eq. (12) are

$$\Delta(\infty)=1,\quad \Delta'(\infty)=0,\quad \Delta''(\infty)=0. \tag{13}$$

Eq. (12) with the initial conditions (13) has to be solved numerically. The numerical procedure requires, however, the knowledge of an approximate analytical solution at infinity. The details of it are given below.

In the case of $X\to\infty$ (see Fig. 1(b)), Eq. (13) can be simplified taking into account that the curvature of the liquid film can be approximated by the second derivative since the first derivative is negligibly small. Then Eq. (12) reduces to the form

$$\Delta'''-\alpha^{-1/2}(\Delta^{-3}-1)+\beta\Delta^{-3}\Delta'=0. \tag{14}$$

However, this equation cannot be solved analytically. It was shown in [11] that for very large X (i.e. $X\to\infty$) the film thickness may be approximated by the function:

$$\Delta(X)=1+Y(X), \tag{15}$$

where $Y(X)$ has to satisfy the conditions:

$$Y(X)\ll 1 \quad\text{and}\quad \lim_{X\to\infty} Y(X)=0, \tag{15a}$$

so we can arrive at the approximations [11]:

$$\Delta^3=(1+Y)^3\approx 1+3Y, \tag{16}$$

and

$$Y'''(1+3Y)\approx Y'''. \tag{17}$$

Since

$$\Delta'=Y' \quad\text{and}\quad \Delta'''=Y''',$$

then Eq. (14) reduces to the linear equation

$$Y'''+\beta Y'+3\alpha^{-1/2}Y=0, \tag{18}$$

with the characteristic equation:

$$\chi^3+\beta\chi-3\alpha^{-1/2}=0. \tag{19}$$

Taking the above into account the solution of Eq. (14) is given as

$$\Delta(X)=1+Y(X)=1+\exp(\chi X), \tag{20}$$

where χ is the only real root of the characteristic equation (19), namely:

$$\chi=\left[-\frac{3}{2\sqrt{\alpha}}+\frac{1}{18}\sqrt{\frac{3(243+4\alpha\beta^3)}{\alpha}}\right]^{1/3} -\frac{\beta}{3}\left[-\frac{3}{2\sqrt{\alpha}}+\frac{1}{18}\sqrt{\frac{3(243+4\alpha\beta^3)}{\alpha}}\right]^{-1/3}. \tag{20a}$$

Now we can determine the starting point $(X_{st},\ Y_{st})$ of the numerical solution of Eq. (12). For the assumed small value of Y_{st} (e.g. the film thickness differs by 0.1% from that at infinity):

$$Y_{st}=0.001;\quad X_{st}=\frac{1}{\chi}\ln Y_{st}, \tag{21}$$

and

$$\Delta(X_{st})=1+Y_{st};\quad \Delta'(X_{st})=\chi\ \exp(\chi X_{st});\quad \Delta''(X_{st})=\chi^2\ \exp(\chi X_{st}). \tag{21a}$$

It is convenient to introduce the dimensionless pressure gradient P in the liquid phase. For $X\to 0$, the dimensionless pressure gradient $P\to 1$, since the pressure term is balanced by the gravity term in the momentum equation (the other terms vanish) as it was shown by Butrymowicz [12]. For $X\to\infty$ the pressure gradient P approaches zero because the curvature disappears. Generally, the flow domain may be divided into:

- Hydrostatic region, $X\leqslant X_M$ ($P\to 1$ for $X\to X_O$).
- Dynamic region, $X>X_M$ ($P\to 0$ for $X\to\infty$).

For $X=X_M$, the curvature should reach its maximum value and then decrease. However, the solution of Eq. (12) does not satisfy such a curvature distribution because the calculated curvature increases monotonously. This part of the solution for the strip does not account for the presence of the tube. Therefore, in order to be in agreement with the physical situation, the sign of the curvature gradient changes, i.e. for $X<X_M$ we have

$$\frac{dp}{dx}=+\sigma\frac{d\kappa}{dx}. \tag{22}$$

Due to the large thickness of the condensate film, it is assumed that for $X<X_M$ the gravity force is balanced by the pressure force due to surface tension (hydrostatic region). The Eq. (12) with the help of Eq. (22) takes the following form

$$\Delta'''-3\alpha\Delta'\Delta''^2(1+\alpha\Delta'^2)^{-1}-(1+\alpha\Delta'^2)^{3/2}\alpha^{-1/2}=0. \tag{23}$$

The point X_M of maximum curvature can be deter-

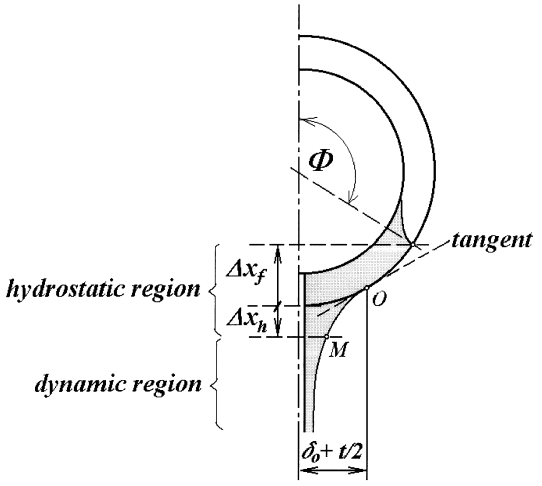

Fig. 2. Hydrostatic and dynamic regions on the strip. Geometrical condition of tangency of the liquid film to the tube. O—point of tangency, M—point of maximum film curvature.

mined by an iterative procedure because for each point $X = X_M$, there is only one point, i.e. $X = X_O$, which satisfies the geometrical condition of tangency of the condensate film to the tube, as it is depicted in Fig. 2. This condition can be described in dimensional form as

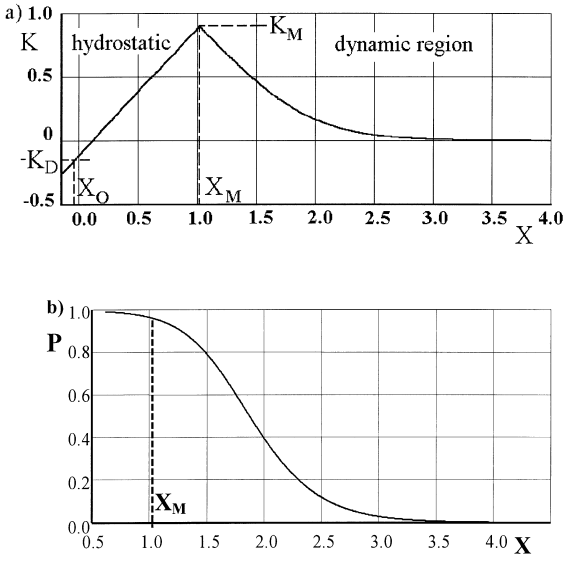

Fig. 3. Examples of dimensionless quantities distribution along the strip for Freon CFC-11, saturation temperature 40°C, $\Gamma = 7.67 \cdot 10^{-3}$ kg/(m·s), $D = 14.0$ mm and strip thickness 1.0 mm. (a) The dimensionless film curvature K distribution. (b) The dimensionless pressure P distribution.

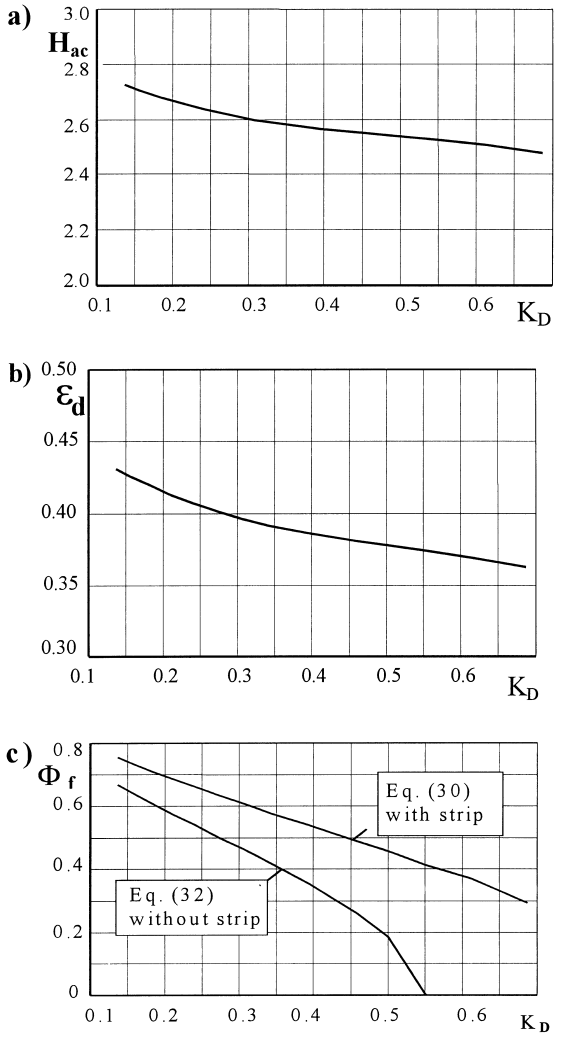

Fig. 4. The exemplary effect of dimensionless tube curvature on the important model parameters (water, $\gamma = 1.213 \cdot 10^5$, $K_c = 3.634$). (a) Dimensionless active strip height. (b) Drainage parameter. (c) Flooding angle.

$$\delta_O + \frac{t}{2} = \frac{D}{2} \sin\left(\arctan(\delta') - \frac{\pi}{2}\right). \tag{24}$$

The above equation can be transformed into the following dimensionless form

$$K(X_O) = \frac{\cos(\arctan(\alpha^{1/2}\Delta'(X_O)))}{\alpha^{1/2}\Delta(X_O) + \tau} = -K_D. \tag{25}$$

Examples of distributions of the dimensionless film curvature and dimensionless pressure along the strip calculated according to the presented model are shown in Figs. 3(a) and (b).

Having had the pressure distribution in the condensate film it is possible now to calculate the active

height of the strip H_{ac} and the flooding angle Φ_f. The first quantity is shown in Fig. 4(a). It was obtained by assuming that this height corresponds to the point where the dimensionless pressure gradient $P = 0.01$.

The pressure p in the liquid phase at the point x_M can be expressed as (see Fig. 2)

$$p = p_s - \Delta p_f + \rho g(\Delta x_f + \Delta x_h), \tag{26}$$

because this point belongs to the hydrostatic region where the gravity force is balanced only by the surface tension. Quantities Δx_f and Δx_h are defined in Fig. 2.

The pressure difference Δp_f between the vapour and the condensate film in the interfin channel may be calculated with the aid of the formula developed by Honda et al. [5]

$$\Delta p_f = \frac{\sigma}{W_t/2}\cos\ \theta, \tag{27}$$

valid when

$$W_t \leq 2\frac{\cos\ \theta}{1-\sin\ \theta}H_f. \tag{27a}$$

On the other hand, at the point x_M the pressure p can be obtained from the Laplace and Young equation

$$p = p_s - \sigma\kappa(x_M). \tag{28}$$

Combining Eqs. (26)–(28) one can get

$$2\frac{\sigma\ \cos\ \theta}{W_t} = \rho g\frac{D}{2}(1+\cos\ \Phi) + \rho g\Delta x_h + \sigma\kappa(x_M). \tag{29}$$

With the use of Eq. (29), the dimensionless flooding angle Φ_f is expressed finally by the formula

$$\Phi_f = \frac{1}{\pi}\arccos(\varepsilon(1-\varepsilon_d)-1), \tag{30}$$

where

$$\varepsilon = K_D K_c, \tag{30a}$$

$$\varepsilon_d = \frac{K_m + \Delta X_h}{K_c}. \tag{30b}$$

The dimensionless curvatures K used in Eqs. (30a) and (30b) correspond, respectively, to the curvature of the condensate in the interfin channel K_c, curvature of the tube K_D, and maximum curvature of the strip K_M

$$K_c = 2\ \cos\ \theta\frac{a}{W_t},\quad K_D = 2\frac{a}{D},$$
$$K_M = K(X_M) = a\kappa(x_M),\quad \Delta X_h = \frac{\Delta x_h}{a}. \tag{31}$$

The coefficient ε_d defined by Eq. (30b) may be named as a drainage parameter. It describes the influence of the tube and strip geometry as well as the physical condensate properties on the drainage effect. The solid strip increases the flooding angle. In the case of absence of the strip the coefficient $\varepsilon_d = 0$, thus, Eq. (30) reduces to the form:

$$\Phi_f = \frac{1}{\pi}\arccos(\varepsilon - 1). \tag{32}$$

As expected, Eq. (32) coincides with the one derived by Honda et al. [5] for the tube without the strip. It is, therefore, shown that Eq. (30) is of general form and is valid for both cases: tubes with and without the solid strips.

Having had the flooding angle it is possible to calculate the heat transfer rate for the finned tube. It was shown in [13] that heat transfer on the finned tube (with or without the strip) can be described by the general formula

$$Nu = 0.725(Ga\ Pr\ Ku)^{0.25}\Omega\Phi_f. \tag{33}$$

One can find details of obtaining Eq. (33) in [13]. The factor Ω reflects the heat transfer enhancement due to the fin geometry. The second factor—flooding angle Φ_f takes into account the effect of the condensate retention. Taking into account that the Nusselt number Nu depends on the dimensionless flooding angle and this angle depends on the heat flux, an iterative procedure is required for the calculation of this quantity.

3. Theoretical results and discussion

Having the model of the solid drainage strip, it is now possible to discuss the influence of some geometrical parameters on the drainage process. Fig. 4(b) shows the effect of dimensionless tube curvature on the drainage parameter ε_d. The effect of the dimensionless tube curvature on the flooding angle, including the influence of both dimensionless parameters ε and ε_d, is presented in Fig. 4(c). It is seen that the difference in the flooding angles for tubes with and without the strip increases with the increasing tube curvature. This means that the influence of the parameter ε on the flooding angle is greater in comparison with the drainage parameter ε_d. From the above considerations one can conclude that the use of the solid drainage strip is more profitable for tubes with small outer diameters. Most of the commercially available refrigeration and heat pump condensers are equipped with the tubes of diameter within the range of 12–20 mm, so the use of the solid strip can improve the drainage process in the majority of practical applications.

It is very interesting to compare the solid strip model Eq. (30) with the only known correlation of the flooding angle for the case obtained by Yau et al. [9]

Table 1
Dimensions of investigated tubes

Parameter	Unit	Adiabatic conditions				Condensation conditions		
		Tube 1	Tube 2	Tube 3	Tube 4	Tube 5	Tube 6	Tube 7
Outer diameter	mm	12	18	40	18	14.0	25.0	14.0
Inner diameter	mm	–	–	–	–	10.0	19.0	10.0
Fin height	mm	1.5	1.0	1.0	1.0	0.5	–	–
Fin thickness	mm	1.0	1.0	1.0	0.0	0.5	–	–
Fin pitch	mm	2.5	2.5	2.5	1.0	1.0	–	–
Fin density	items/m	400	400	400	1000	1000	–	–
Fin tip half angle	rad	0.0	0.0	0.0	0.0	0.0	–	–
Material	–	Brass	Brass	Brass	Brass	Brass	Brass	Brass

$$\Phi_f = \frac{1}{\pi}\text{arc}\cos(0.415\varepsilon - 1). \quad (34)$$

It was shown in [11] that both equations [i.e. (30) and (34)] are identical if the coefficient $\varepsilon_d = 0.585$. Thus, the above correlation may be thought of as the valid one for the conditions of the coefficient ε_d which differs only slightly from its average value of 0.585.

4. Apparatus and procedure

Experiments were conducted on two special stands designed to investigate separately: liquid flooding under adiabatic conditions and condensation heat transfer in the case of condensate drainage.

Details of the first stand are described in [14]. In order to evaluate the flooding angle and the capillary constant of water, an optical measuring system was used. The tested tube was wetted with water with the help of a special wetting system. The flow rate of supply water was established by measuring the time change of its volume in the calibrating tank.

The phenomenon of flooding of inter-fin channels is governed, first of all, by surface tension and gravitational forces, and also by the geometry of the finned tube. In order to conduct the investigations with due care it is necessary to determine as accurately as possible the capillary constant of water flooding the finned tube. The pendant drop method, slightly modified by the authors, was used for this purpose [14]. Needless to say, the capillary constant can change considerably with the presence of additives into the working medium.

Dimensions of the brass finned tubes used in the investigations are presented in Table 1. The tubes have the perpendicular profiled fins. Drainage strips were made of sheet brass 1 mm thick. They were fitted to the tubes by pressing into special slots. Strips 4, 10 and 20 mm in height were used in the course of the investigations. The tubes were carefully cleaned before being measured so as to remove dirt and grease from their surface.

A schematic diagram of the second experimental stand for condensation heat-transfer of Freon CFC-11 is presented in Fig. 5. The rig consists of two main parts—the condenser 2 with a tested tube mounted inside and the vapour generator 8. The condenser, 135 mm in outer diameter and 275 mm in total length is equipped with six glass windows. Other elements of the condenser are: a dish to collect the condensate, a gear to lift the drainage strip, mano-vacuumeter (these are not indicated in Fig. 5) and air purging valve 7. Thanks to the lifting gear the drainage strip can be

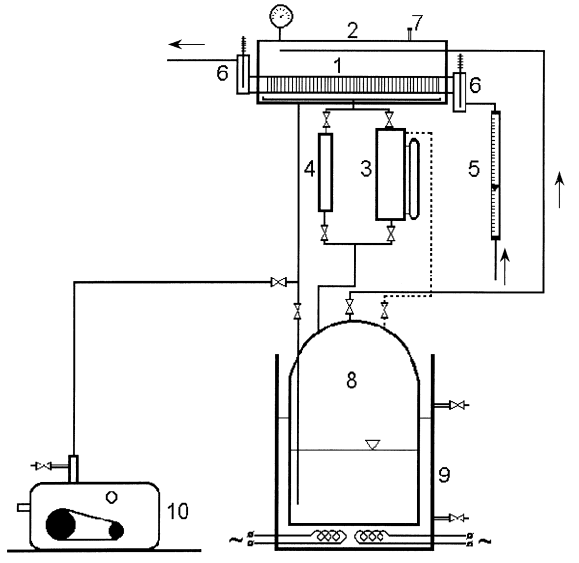

Fig. 5. A schematic of stand for investigations of condensation heat transfer on a single horizontal tube: 1. test tube; 2. condenser; 3. calibrating tank; 4. dehydrator; 5. rotameter; 6. water temperature measurement tank; 7. air purging valve; 8. vapour generator; 9. hot water container; 10. vacuum pump.

fitted tight to the bottom of the tube or at any distance from it. Only the liquid condensing at the tested tube can flow down to these tanks, the remaining condensate flows down another separate pipeline to the vapour generator placed in a hot water container 9 equipped with four heaters with a power of 0.8 kW each. The rotameter 5 is used to measure the flow rate of cooling water. Additionally, in order to equalise the temperature of cooling water, water temperature measurement tanks 6 were installed at both sides of the condenser. A turbulizer was placed inside the investigated tube so as to intensify heat transfer on the water side.

The following quantities were measured in the course of investigations: the wall average temperature of the investigated tube, vapour saturation temperature and water temperature before and behind the condenser with the help of thermocouples, the vapour pressure using a mano-vacuumeter, condensate volume and volumetric flow rate—using a stop-watch and calibrating tank and water volumetric flow rate—with the help of rotameters.

The average surface temperature of the tested tube on the vapour side was determined as the arithmetic mean of local read from thermocouples. In order to install them the longitudinal grooves were machined along the tube axis. The thermocouples were placed in tubes with an inner diameter equalling that of their diameter (0.5 mm) and then they were soldered and the fins were machined on the tube. The thermocouples were installed in two cross-sections and placed circumferentially at every 90° for tube 6 and 120° for tubes 5 and 7. Dimensions of the test tubes are displayed in Table 1. The drainage strip used in the investigations was made of sheet copper 1 mm thick. The height of the strip was 4 mm. The test rig as well as the measuring procedure is described in more detail in [12].

5. Results for adiabatic conditions

It follows from the theoretical model that the effect of the drainage strip depends on the outer diameter of the tube and increases with the decreasing diameter. Therefore, the investigations were conducted for tubes with the same fin geometry but a different diameter.

The conditions of adiabatic measurements differed from those of the film condensation. Therefore, the contact angle θ_w, which equals zero in the case of film condensation, should be taken into account in the formula to determine the flowing angle. The dimensionless curvature of the meniscus in the inter-fin channel can be expressed in the form similar to (31)

$$K_c = 2\frac{a}{W_t}\cos(\theta + \theta_w). \tag{35}$$

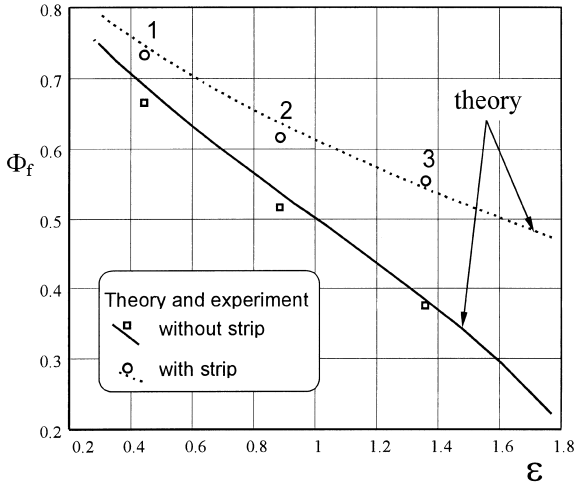

Fig. 6. Theoretical and experimental values of the dimensionless flooding angle as a function of parameter ε for water, $\Gamma = 7.5 \cdot 10^{-3}$ kg/(m·s), contact angle $\theta_w = 32°$. 1. $D = 40$ mm, 2. $D = 18$ mm, 3. $D = 12$ mm.

The above amendment can be obtained from geometrical relations. The contact angle for the test tube was estimated before measurements of the flooding angle. The investigations revealed that the mass flow rate Γ does not affect the flooding angle.

Theoretical and experimental data of the flooding angle for water are presented in Fig. 6. A good agreement between theory and experiment is obtained. The experimental data also confirm that for tubes having lower diameters the drainage effect is larger. This important result for practical application has not been proved experimentally before.

Besides measurements of the flooding angle, we also measured the profile of the liquid meniscus at the strip—using an optical system [14]. Discrete distributions of the film thickness down the drainage strip were determined from photographs taken in the plane perpendicular to the tube axis. The photographs were magnified to appropriate dimensions so as to assure high resolution of the image. The investigations under conditions of continuous wetting of the tube were carried out for tube 4 with a strip 10 mm in height. Based on the given measured values, a continuous distribution of the film thickness can be approximated with the help of an exponential function derived analytically if $\delta' \ll 1$:

$$\Delta(X) = C_0 + C_1 \exp(C_2 X), \tag{36}$$

where coefficients C_0, C_1 and C_2 were found in a numerical way. Given the continuous distribution of the film thickness, one can find the distribution of the non-dimensional film curvature as

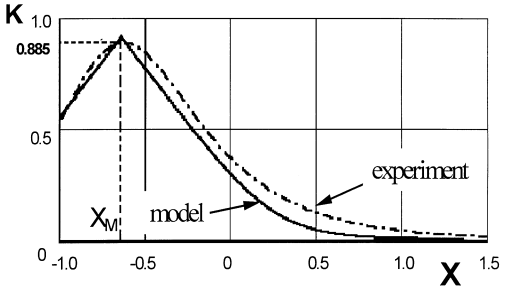

Fig. 7. The non-dimensional film curvature distribution on the strip 10 mm in height for tube 4 in adiabatic conditions—water, $\Gamma = 7.5 \cdot 10^{-3}$ kg/(m·s).

$$K(X) = \frac{\Delta'' \alpha^{1/2}}{(1 + (\Delta')^2 \alpha)^{3/2}}. \tag{37}$$

The distribution of the film curvature for tube 4 is shown in Fig. 7. The experimental values of curvature K_m (at point M) is equal to 0.885, whereas calculated from the model it is 0.909. This sounds like a reasonable agreement.

6. Results of condensation heat transfer

In order to validate the model of the solid drainage strip in respect to heat transfer during condensation of vapour on a finned tube separate investigations were

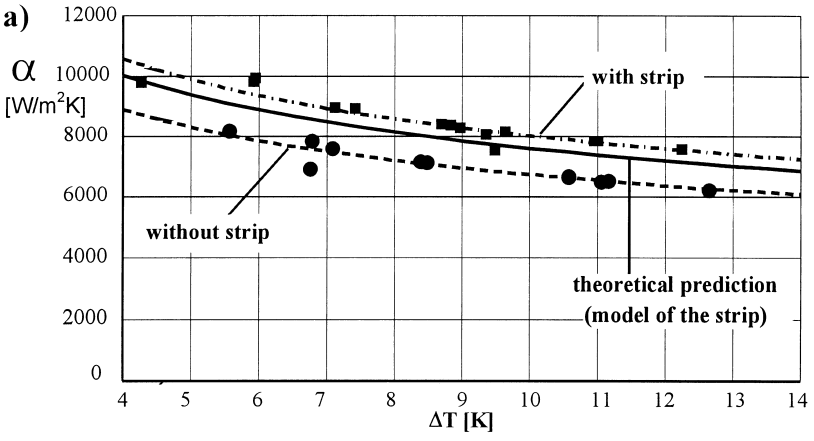

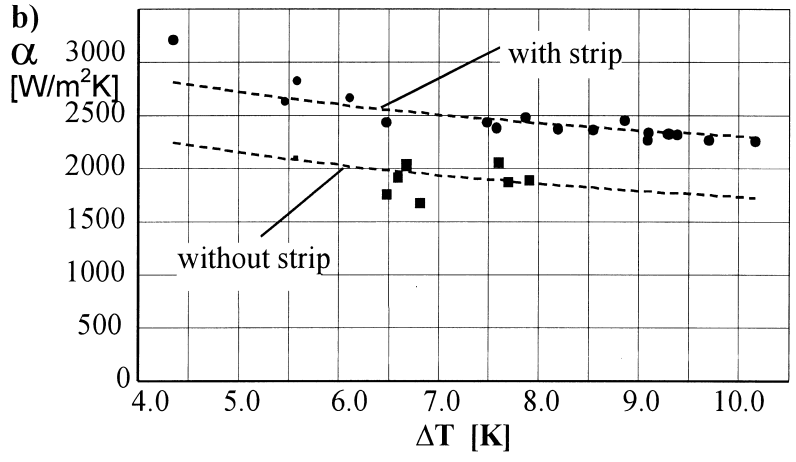

Fig. 8. The heat-transfer coefficient for the investigated tubes. Dashed lines correspond to the best fit of the experimental data. (a) Integral-fin tube 5 with and without a strip. (b) Unfinned tube 6 with and without a strip. (c) Unfinned tube 6 with the strip fitted tight and a distance of 1 mm under the tube. (d) Unfinned tube 7 with and without a strip.

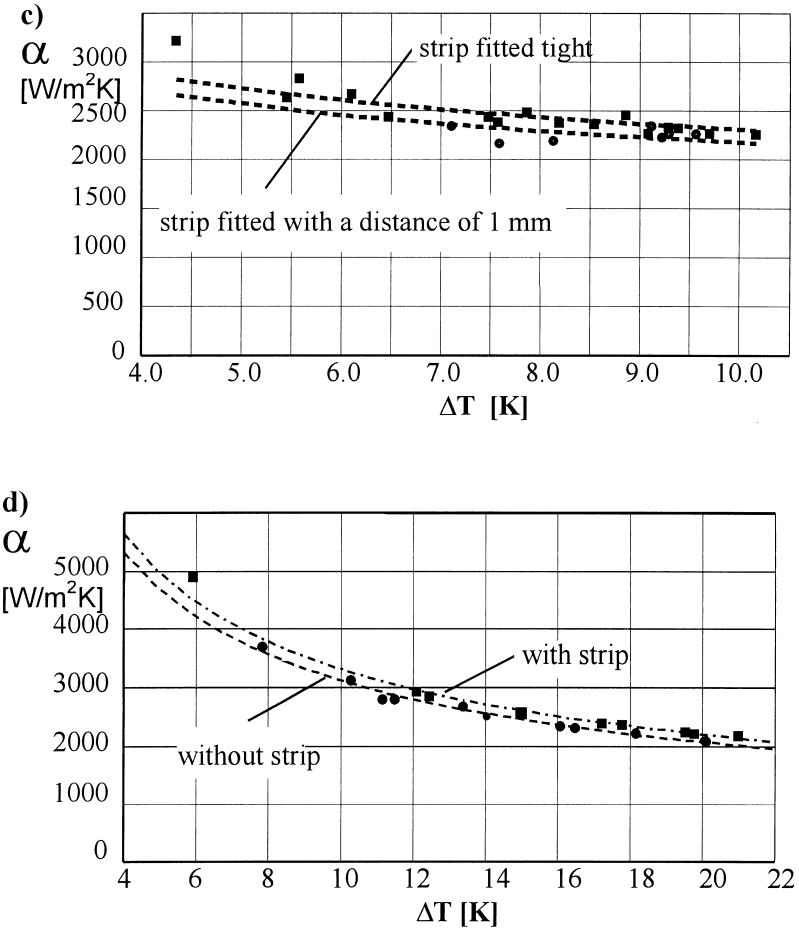

Fig. 8 (*continued*)

carried out. The research was also extended to unfinned tubes equipped with solid drainage strips.

The data were recorded once a steady state was achieved. Basically from all data points the only ones taken into account were when the difference of the heat flux calculated from heat balances on the water and vapour sides did not exceed 15%. For most data points this difference was below 5% owing to careful measuring, appropriate scaling and zeroing of the rotameter and the whole test rig. A detailed description of the calculation procedure, zeroing of the test rig and correction of some measured quantities is presented in [12].

We begin with the discussion of the results for the horizontal integral-fin tube denoted as 5, Table 1. They are shown in Fig. 8(a). As a result of the solid strip application, the heat transfer coefficient increased by as much as 19%, compared to the tube without a strip. On the other hand, it follows from the calculations based on the strip model that the heat transfer coefficient should increase by 13%. The discrepancy between the theoretical and experimental heat transfer coefficient is partially due to simplifying assumptions in the theory. In Eq. (33) the heat transfer at the part of the finned tube flooded by the condensate is entirely neglected. Unlike in the case of adiabatic conditions it was impossible to measure the capillary constant during heat transfer investigations. Taking into account the above notes, the experimental results fall well within the predictions of the model presented above.

As mentioned before, the condensate drainage from a horizontal unfinned tube equipped with a solid drainage strip is also due to the region of low pressure in the condensate layer formed at the very bottom of the tube.

The experimental investigations were carried out for unfinned tubes denoted as 6 and 7, whose dimensions are listed in Table 1, for a number of configurations of the strip. Measured values of the heat-transfer coefficient for the unfinned tube 6 without a strip and with the strip mounted tight to the tube are presented in

Fig. 8(b). Fig. 8(c) shows the measured values of the heat-transfer coefficient for the unfinned tube 6 with the strip fitted tight and at a distance of 1.0 mm.

There are several useful conclusions from these experiments. First, solid drainage strips can also be used for bare tubes to effect enhancement of heat transfer. Secondly, the precision of mounting of the strip to the bottom part of the tube is not that important.

Results of measurements of the heat-transfer coefficient carried out for the unfinned tube 7, with and without a strip, are depicted in Fig. 8(d). In this case the heat transfer coefficient for the tube with the strip fitted tight only increased by 6%, compared to the tube without a strip.

7. Concluding remarks

It is shown in the paper that the enhancement of condensate drainage can be obtained by means of a solid strip. Due to the action of the strip the condensate retained between the fins is drained off, leaving more surface available for heat transfer. The model of the solid strip has been proposed and the importance of its parameters has been discussed. The most important parameter in the model is the drainage parameter ε_d. It reflects the influence of fin and tube geometry as well as the physical properties of the condensate on the drainage process. It has been found in the course of numerical calculations based on the presented model that:

1. The drainage parameter ε_d decreases with the increasing tube curvature.
2. The geometrical parameter ε and the drainage parameter ε_d have a mutually opposing effect on the drainage process. The use of the solid drainage strip should be more profitable for tubes with small outer diameters.
3. The active height of the strip is limited and approximately equal 2–4 capillary constants. This height is a weak function of tube curvature or heat flux.
4. The flooding angle Φ_f is scarcely influenced by the strip thickness and heat flux.

Further conclusions can be drawn from the analysis of experimental results:

5. The experiments carried out under adiabatic conditions speak entirely in favour of the theoretical model of the solid drainage strip. The particular ones carried out for different tube diameters, leaving the fin geometry unchanged, confirm the theoretically predicted effect of the outer tube diameter on the condensate drainage process.
6. The application of the solid drainage strip increases the heat transfer coefficient α. This increase amounts to 19% for the investigated integral-fin tube.
7. The heat transfer coefficient also increases for unfinned tubes equipped with the solid drainage strip. Its increase depends on the tube diameter. For an unfinned tube 25 mm in outer diameter, the heat transfer coefficient increases by 25%, for the tube 14 mm in diameter it increases by only 6%. The increase of the heat transfer coefficient is due to a phenomenon similar to that described for the case of finned tubes.
8. Mounting the strip at some distance under the tube does not intensify nor lessen the heat transfer. This implies that the application of the solid drainage strip does not involve particular technological requirements.

Acknowledgement

This paper was supported by the Polish Committee for Scientific Research, Grant No. PB 0467/P4/94/07 and Grant No. 8T10B 00810.

References

[1] R.L. Webb, T.M. Rudy, M.A. Kedzierski, Prediction of the condensation coefficient on horizontal integral-fin tubes, ASME J. Heat Transfer 107 (1985) 369–376.
[2] K.K. Yau, J.R. Cooper, J.W. Rose, Effect of fin spacing on the performance of horizontal integral-fin condenser tubes, ASME J. Heat Transfer 107 (1985) 377–383.
[3] A.S. Wanniarachchi, P.J. Marto, J.W. Rose, Film condensation of steam on horizontal finned tubes: effect of fin spacing, ASME J. Heat Transfer 108 (1986) 960–966.
[4] T. Adamek, R.L. Webb, Prediction of film condensation on horizontal integral fin tubes, Int. J. Heat Mass Transfer 33 (1990) 1721–1735.
[5] H. Honda, S. Nozu, K. Mitsumori, Augmentation of condensation on horizontal finned tubes by attaching a porous drainage plate, in: Y. Mori, W-J. Yang (Eds.), Proceedings of ASME–JSME Thermal Engineering Joint Conference, 3, 1983, pp. 289–296.
[6] T.M. Rudy, R.L. Webb, An analytical model to predict condensate retention on horizontal integral-fin tubes, ASME J. Heat Transfer 107 (1985) 361–368.
[7] H. Honda, S. Nozu, Effect of drainage strips on the condensate heat transfer performance of horizontal finned tubes, in: Proceedings of International Symposium on Heat Transfer, 2, 1985, pp. 455–462, Paper No. 85-ISHR-II-32.
[8] P.J. Marto, A.S. Wanniarachchi, D. Cakan, J.W. Rose, Enhancement of steam condensation on a horizontal finned tube by using drainage strips, in: Proceedings of the 2nd UK National Heat Transfer Conference, Glasgow, Scotland, 1, 1988, pp. 603–616.

[9] K.K. Yau, J.R. Cooper, J.W. Rose, Horizontal plain and low finned condenser tubes—effect of fin spacing and drainage strips on heat transfer and condensate retention, ASME J. Heat Transfer 108 (1986) 946–950.

[10] A.L. Yemielianov, V.O. Mamtshenko, S.V. Hizniakov, Intensification of heat transfer during condensation of freons on horizontal tube bundles, Kholodilna Technika 9 (1989) 48–52 (in Russian).

[11] D. Butrymowicz, M. Trela, Prediction of the flooding angle on a horizontal finned tube fitted with the drainage strip, Archives of Thermodynamics 16 (3–4) (1995) 145–163.

[12] D. Butrymowicz Experimental and theoretical investigations of condensation on integral-fin tubes with condensate drainage (in Polish), PhD thesis, Institute of Fluid-Flow Machinery of Polish Academy of Sciences, Poland, Gdańsk, 1997.

[13] D. Butrymowicz, M. Trela, Investigations of heat transfer on a horizontal fin-tube fitted with the drainage strip, Archives of Thermodynamics 18 (3–4) (1997) 25–48.

[14] D. Butrymowicz, M. Trela, E. Ihnatowicz, The measurement of the capillary constant by the pendent drop method, in: Proceedings of the International VI Symposium "Heat Transfer and Renewable Energy Sources", Szczecin-Świnoujście, Poland, 1996, pp. 61–68.